Challenges with Optically Transparent Patch Antennas

Jason R. Saberin and Cynthia Furse

Department of Electrical and Computer Engineering
University of Utah
Salt Lake City, UT 84119 USA
E-mail: jasonsaberin@gmail.com; cynthia.furse@utah.edu

Abstract

In this paper, antennas made out of transparent conducting oxides (TCOs) are explored. The optical transparency of transparent conducting oxides is achieved through thin-film depositions on substrates. However, thin-film depositions create a new set of electrical challenges that require a full understanding of semiconductor physics. This work looks into the governing equations that limit light transmission, absorption, and reflection through a transparent conductor, along with the electrical conductivity and antenna efficiency of transparent-conducting-oxide thin-film patch antennas.

Keywords: Microstrip antennas; patch antennas; transparent antennas; indium tin oxide; thin films

1. Introduction

Transparent conductive materials have been prepared with oxides of tin, indium, zinc, and cadmium [1]. These semiconductor transparent conducting oxides (TCOs) are employed in a wide spectrum of applications, such as solar cells, electromagnetic shielding, and touch-panel controls [1]. Notably, there has been little commercial application of transparent conducting oxides in antenna design. Attempts have been made to create transparent patch antennas for automobile windshields and solar cells [2-6]. Many papers on this subject expressed the inability of achieving high gains (more than 2 dB) [5] and reduced efficiencies of microstrip antennas, compared to antennas that are not near a ground plane [2], such as a dipole in free space. Previous transparent-antenna research has offered little insight into the use and limitations of transparent-conducting-oxide antennas in general. There has also been little insight into what range of conductivity and transparency can be expected from today's materials, and how that impacts antenna performance for different frequency bands. This paper explores the tradeoffs and discusses the implementations for antenna design using today's materials, and as transparent-conducting-oxide materials mature.

In order to better understand the importance of these material-science constraints and how they impact transparent-antenna design, this paper looks at transparent conductors in a language that can be understood by antenna engineers. In this effort, we examine various issues that plague thin-antenna design using thin-film transparent conductors, including skin-depth losses, ground losses, and surface losses. Skin-depth losses are introduced by the requirement of high optical transparency, which requires thin transparent-conducting-oxide depositions, reducing antenna efficiency. Ground-effect losses in the ground plane of patch antennas further reduce efficiency. Both of these issues, coupled with the relatively low conductivity of transparent conducting oxides [7], (approximately 8×10^5 S/m for indium tin oxide, ITO) can cause significant increases in the surface resistance of the microstrip patch, and resultant lower efficiency. Taking into consideration all of these effects, this work will evaluate 1) the necessary parameters of a transparent material for antenna design, 2) the type of losses associated with thin-film depositions due to ground- and skin-effect losses in microstrip-patch antennas, and 3) design considerations to mitigate the antenna's surface resistance and to improve efficiency. The first item is addressed by a thorough explanation of transparent-conducting-oxide material physics, which will illustrate how to manipulate free-electron doping and electron mobility to improve transparency and maximize conductivity. The second item introduces an empirical equation to approximate surface resistance due to skin and ground losses. The third item evaluates the expected optical transparency and radiation efficiency of today's transparent conducting oxides, and those that we may hope to see in the future. It may also be noted that many of the concepts in this paper apply to the design of antennas with other imperfectly conducting materials, such as textiles.

doping, the optical and conductive properties may be simply described by using Drude's model [9], presented in the following paragraph.

Drude's model expresses the dielectric property of a material as a function of frequency:

$$\epsilon(\omega) = \epsilon_\infty - \frac{\omega_p^2}{\omega^2 + \frac{j\omega}{\tau}}, \tag{1}$$

where the term ϵ_∞ is the high-frequency dielectric constant contributed by the valence electrons, and τ is the electronic relaxation time. The plasma frequency, ω_p, can be determined by

$$\omega_p = \left(\frac{N_e q^2}{\epsilon_\infty \epsilon_0 m^*} - \frac{1}{\tau^2} \right)^{\frac{1}{2}}, \tag{2}$$

where N_e is the electron density of the transparent conducting oxide in m^{-3}, q is the electron charge in Coulombs, and τ is the electronic relaxation time. From Equation (2), it is noted that the electronic relaxation time, τ (also referred to as electron mobility, $\mu_e = q\tau_0 / m^*$), has very little influence. It is thus considered to have a negligible effect on the plasma frequency, leaving the electron density, N_e, as the dominant factor that determines the plasma frequency of the transparent conducting oxide, illustrated in Figure 2. We can also define an expression to form a single effective frequency-dependent conductivity expression, given by the Drude form

$$\sigma(\omega) = \frac{N_e q^2 \tau}{m^*} \frac{1}{1 + j\omega\tau}. \tag{3}$$

In order to maximize optical transmission of the whole visible electromagnetic spectrum ($\lambda_{visible}$ = 400 nm to 700 nm) through the material, the plasma frequency must be below the lowest visible wavelength ($2\pi/\omega_p < \lambda_{visible}$). If the plasma frequency is set to be barely below the lowest visible wavelength, it is found that the electron density, N_e, must satisfy the following relationship:

$$N_e < \frac{4\pi^2 \epsilon_\infty m^*}{\mu_0 q^2 \lambda_{visible}^2}, \tag{4}$$

where μ_0 is the magnetic permeability of free space. Equation (4) will serve as a guideline for the doping of free electrons in the transparent material. To allow a small margin of error for visible transmission, it is recommended that we use a material with a plasma wavelength of just over $\lambda_p = 1\,\mu\mathrm{m}$ (near infrared). The power reflection for optical frequencies, $R(\omega)$, of a uniform transparent-conducting-oxide deposition (dielectric slab) is defined as

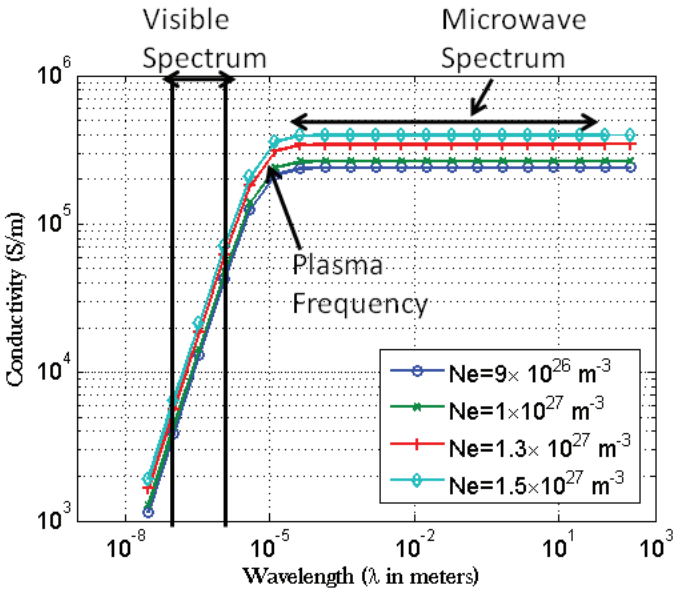

Figure 2. A typical transparent conducting oxide conductivity as a function of wavelength for frequencies ranging from the visible spectrum through the microwave regime.

$$R(\omega) = \left| \frac{\sqrt{\epsilon(\omega)} - 1}{\sqrt{\epsilon(\omega)} + 1} \right|^2. \tag{5}$$

For frequencies much lower than the plasma frequency, ω_p, the normal-incidence transmission coefficient, $T(\omega) = 1 - R(\omega)$ tends to be close to 0. Alternatively, for frequencies above the plasma frequency, the transmission coefficient increases, and $\lim_{\omega \to \infty} = 1$, depending on the transparent conducting oxide's permittivity values. This transmission coefficient is also dependent on the amount of absorbed energy as it travels through the lossy dielectric slab (the transparent conducting oxide), and its angle of incidence. Further analysis may be required on the effects of transparent-conducting-oxide transmission at oblique transmission angles. At normal angles of incidence, the amount of transmitted absorbed energy is determined by the electromagnetic skin depth, δ, which constrains the electromagnetic wave energy loss as it travels through a thickness t of the transparent conducting oxide. The transmission of light through a transparent conducting oxide is well approximated by

$$T(t) \cong e^{\left(\frac{-2t}{\delta}\right)}. \tag{6}$$

The dual characteristic of light absorption and microwave-energy conduction of the transparent conducting oxide yields two separate equations that determine the skin depth at frequencies where (1) the transparent conducting oxide is a good conductor, but not very transparent: $\omega_p > \omega$, Case 1; and (2) where the transparent conducting oxide is a good conductor and transparent: $\omega_p < \omega$, Case 2; as illustrated below:

Case 1, where $\omega_p > \omega$, $\omega\tau \ll 1$:

$$\epsilon_2 \approx \frac{\omega_p^2 \tau}{\omega} \gg |\epsilon_1|,$$

$$\delta \approx \left(\frac{2}{\omega\mu\sigma}\right)^{1/2};$$

Case 2, where $\omega_p < \omega$, $\omega\tau \gg 1$:

$$\epsilon_2 \approx \frac{\omega_p^2 \tau}{\omega^3 \tau} \ll |\epsilon_1|,$$

$$\delta \approx \frac{2m^*}{Z_\infty q^2}\frac{\omega^2\tau}{N_e};$$

where we assume that $\omega < E_g/\hbar$, $\epsilon_1 \approx \epsilon_\infty$, $Z_\infty = 377/\sqrt{\epsilon_\infty}\ \Omega$, and μ is the magnetic permeability of the transparent conducting oxide. In the second case, the transparency is proportional to the electron mobility, τ. Furthermore, an increase in mobility will ultimately increase both the transparency and skin depth of the transparent conducting oxide [7]. It is also important to observe that an increase in the free electron mass, m^*, will have the same effect. Therefore, the choice of a transparent conducting oxide for antenna design is determined by the material's electron density, N_e; the free electron mobility, μ_e; and the free electron mass, m^*; ultimately dictated by the transparent-conducting-oxide's $(E, \mathbf{k})$ band-structure shape. It is important to note that indium tin oxide is considered a semiconductor, due to its wide bandgap of 3.7 eV.

3. Skin and Ground Effects on Thin-Film Microstrip Antennas

Unlike dipole antennas in free space, the current distribution on the microstrip patch can vary significantly when the width, W, of the patch is much greater than the height, h, $W/h \gg 1$, as seen in Figure 4. This change in current distribution is better understood with the help of the *field equivalence principal* (Huygens' principle) [10]. Under a condition where $W/h \gg 1$, we can assume that the current on the top of the patch ($\mathbf{J}_t$) is much smaller than the current on the bottom ($\mathbf{J}_b$). Under this assumption, the cavity model provides further simplification by considering the current density on the top of the microstrip patch, $\mathbf{J}_t$, to be zero [10]. Moreover, because the ground plane is near the patch, the magnetic current density is maximized on the walls of the cavity, thus doubling the magnetic current density on the perfect-current-density conducting walls.

The increase in magnetic current density in the cavity model results in an increased current distribution on the bottom surface of the microstrip patch, as seen in Figure 3 and Figure 4, where the current-density distribution of a microstrip patch is compared to its width-to-height ratio [11]. This situation implies that the ac resistance of the strip, R_s, at large width-to-height ratios can be as much as twice that for smaller ratios [11]:

$$R_s = R_s, \text{ if } \frac{W}{h} < 1;$$
$$R_s = 2R_s, \text{ if } \frac{W}{h} \gg 1. \quad (9)$$

When using transparent conducting oxides, thin-film deposition on the order of 100 nm to 2 µm is necessary to keep transparency high. However, when depositions are thinner than the skin depth, $\delta = (2/\sigma\omega\mu)^{1/2}$, the surface resistance dramatically changes as a function of thickness, t, compounded by an effective doubling of this resistance for large W/h ratios. Additionally, these losses can be further analyzed with a circuit-equivalent representation of surface impedance, shown in Figure 5.

In good conductors, surface impedance may account for fields outside and inside the conductor. For good conductors with deposition thicknesses much bigger than the skin depth, $t \gg \delta$, the surface-impedance equation, $Z_s = (1+j)(\omega\mu/2\sigma)^{1/2}$, is well defined for calculation of surface losses. However, when dealing with thicknesses that are smaller than the skin depth, $t < \delta$, the surface-impedance equation changes.

In Figure 5, we find that

$$i_2 = v_1 dG = \sigma v dx \quad (10)$$

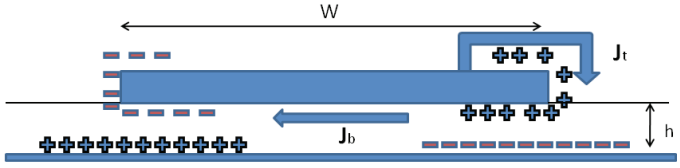

Figure 3. An illustration of the charge and current-density distributions on a patch antenna.

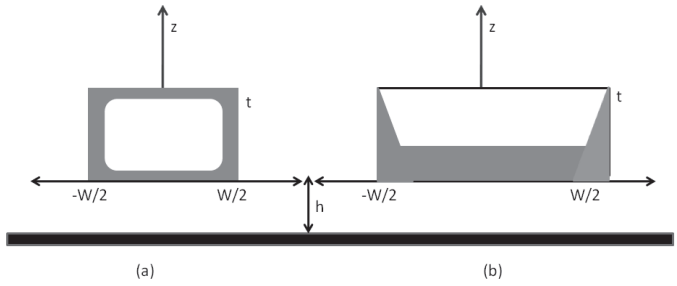

Figure 4. Cross sections of a microstrip current at microwave frequencies where (a) $W/h \ll 1$ and (b) $W/h \gg 1$.

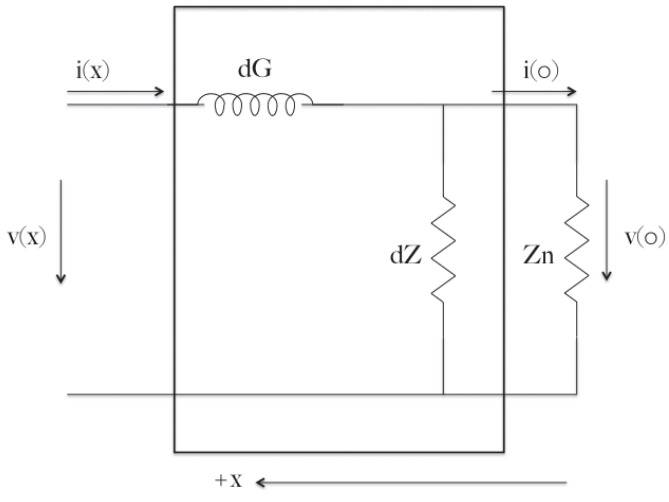

Figure 5. A circuit-equivalent representation of surface impedance.

and

$$v_2 = i_1 dZ = j\omega\mu i_1 dx \,. \tag{11}$$

Hence,

$$Z_s = \frac{v(t)}{i(t)} = \frac{k}{\sigma}\left[\frac{e^{kt} + \dfrac{\sigma Z_\eta - k}{\sigma Z_\eta + k}e^{-kt}}{e^{kt} + \dfrac{\sigma Z_\eta - k}{\sigma Z_\eta + k}e^{-kt}}\right], \tag{12}$$

where

$$\begin{aligned} k &= \sqrt{j\omega\sigma\mu} \\ &= (1+j)\sqrt{\frac{\omega\sigma\mu}{2}} \\ &= \frac{1+j}{\delta}\,. \end{aligned} \tag{13}$$

In most cases, we consider $Z_\eta \gg k/\sigma$. We may then simplify Equation (12) [12]:

$$Z_s = \frac{k}{\sigma}\frac{e^{kt} + e^{-kt}}{e^{kt} - e^{-kt}}\,. \tag{14}$$

Due to an extreme current-density deformation at thicknesses $t \ll \delta$, a full-wave numerical solver may be necessary to properly predict skin and ground effects, and hence surface resistance, for transparent-patch antennas [12]. Additionally, Equations (12) and (14) do not account for additional sources of loss, such as surface roughness, lossy substrate, lossy ground planes, etc.

4. Analysis of TCO Effects on Patch Transparency

In order to better understand the effects of electron mobility, μ_e, and electron density, N_e, on the transparency of a transparent conducting oxide, we will analyze indium tin oxide, a widely used transparent conducting oxide for use in antenna design. Electron mobility and electron density can be controlled through changing oxygen and argon concentrations. Annealing can improve transparency as well as conductivity [1]. Various deposition methods – such as dc sputtering, RF sputtering, thermal deposition, spray pyrolysis, and pulsed laser deposition – may be used for thin-film deposition of indium tin oxide on a substrate [1]. These methods can influence the transparent-conducting-oxide's deposition rate, the uniformity, and the oxide doping. A transparent conducting oxide may be deposited on a variety of optically transparent substrate materials, such as glass and clear fluorocarbon (FEP) film.

Typical values for the permittivity and effective electronic mass of indium tin oxide are $\epsilon_\infty \approx 4.0$ and $m^* = 0.35m_e$ [7]. The electron mobility on high-quality indium-tin-oxide films can reach values of $\mu_e \approx 50\times10^{-4}$ cm^{2}V^{-1}s^{-1}, with a dc scattering time of $\tau_0 \approx m^*\mu_e/q \approx 10^{-14}$ s. Drude empirical approximations suggest that the electronic relaxation time is $\tau \approx 3.3\times10^{-15}$ s. For our example antenna, a glass substrate with a dielectric of $\epsilon_r = 6.0$ and a height of $h = 2.3$ mm was used. The ground plane was copper, and was considered to be a perfect electric conductor (PEC).

In Figure 6, we find that optical transmissions for indium tin oxide were high (greater than 50%) at deposition thicknesses of $t \le 1\,\mu$m or below. The optical transparency of the microstrip patch was not greatly affected by the electron density, but much better transmission of light was achieved if we increased the electron mobility to $\mu_e = 100\times10^{-4}$ cm^{2}V^{-1}s^{-1}, as seen in Figure 7. The decay of the optical transparency was greatly reduced below an electron density of $N_e < 1\times10^{27}$ m^{-3}, keeping optical transparency above 60%. Although transparencies improved with lower electron densities, the electrical conductivity suffered. Increasing electron mobility, on the other hand, increased both the transparency and conductivity.

Table 1 showed that conductivity approximately doubled as electron mobility doubled. The same relationship was observed for the increase of electron density. The near linearity of this relationship gave $\mu_e \propto \sigma$ and $N_e \propto \sigma$.

5. TCO and Antenna Design

In the figures discussed in the following, rectangular microstrip-patch antennas were designed to be resonant from a range of 100 MHz to 10 GHz, with an input impedance of

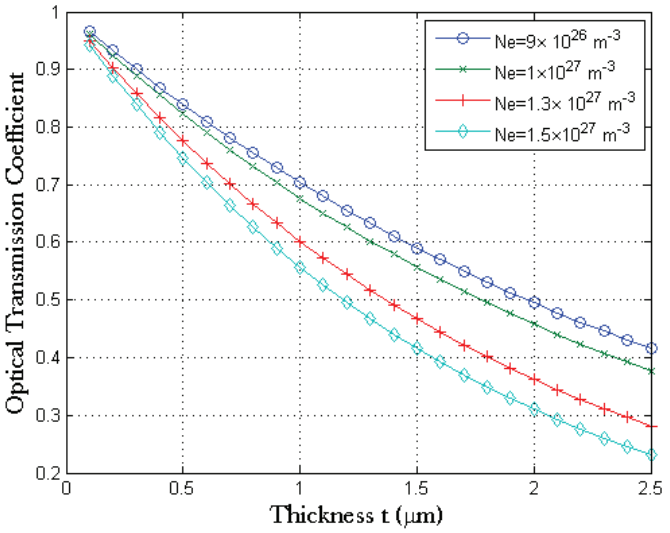

Figure 6. The optical transmission coefficient for $\lambda_0 = 550$ nm light and an electron mobility of $\mu_e = 50\ \mathrm{cm^2V^{-1}s^{-1}}$ for various electron densities, N_e.

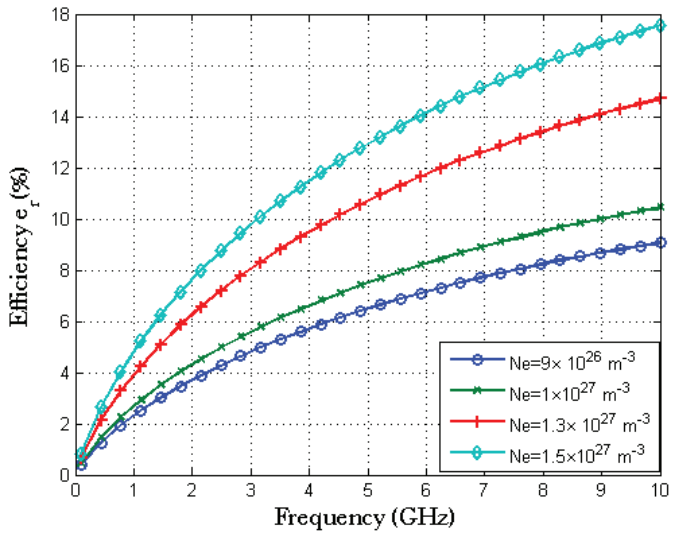

Figure 8. The microstrip-patch efficiency, e_r, for various antennas above a PEC ground with resonant frequencies between 100 MHz and 10 GHz, for an electron mobility of $\mu_e = 50\ \mathrm{cm^2V^{-1}s^{-1}}$.

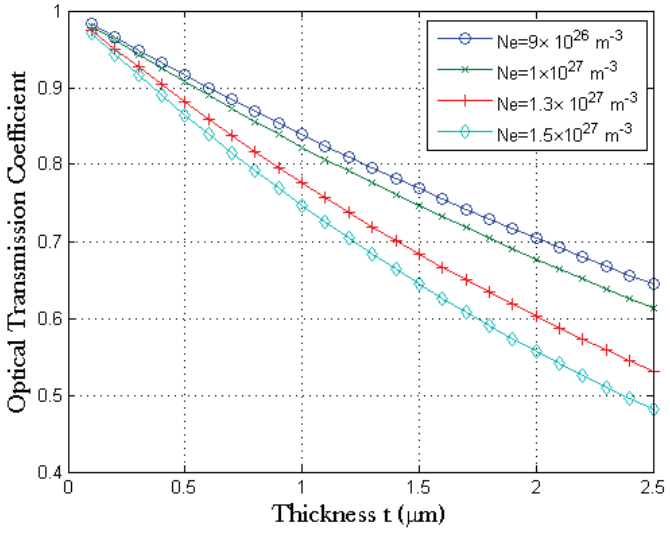

Figure 7. The optical transmission coefficient for $\lambda_0 = 550$ nm light and an electron mobility of $\mu_e = 100\ \mathrm{cm^2V^{-1}s^{-1}}$ for various electron densities, N_e.

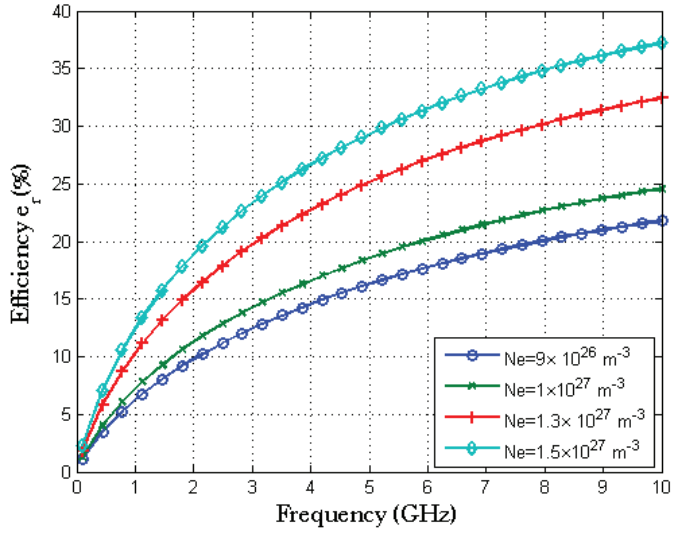

Figure 9. The microstrip-patch efficiency, e_r, for various antennas above a PEC ground with resonant frequencies between 100 MHz and 10 GHz, for an electron mobility of $\mu_e = 100\ \mathrm{cm^2V^{-1}s^{-1}}$.

Table 1. The conductivity of transparent conducting oxides for electron mobilities, μ_e, and various electron densities, N_e.

	$N_e = 9\times10^{26}\ \mathrm{m^{-3}}$	$N_e = 1.3\times10^{27}\ \mathrm{m^{-3}}$	$N_e = 1.5\times10^{27}\ \mathrm{m^{-3}}$
$\mu_e = 50\ \mathrm{cm^2V^{-1}s^{-1}}$	2.4×10^5 S/m	3.4×10^5 S/m	4.0×10^5 S/m
$\mu_e = 100\ \mathrm{cm^2V^{-1}s^{-1}}$	4.8×10^5 S/m	6.9×10^5 S/m	8.0×10^5 S/m

Table 2. The electron mobilities and densities of various transparent conducting oxides.

Transparent Conductor	Mobility, μ_e $\left[\text{cm}^2\text{V}^{-1}\text{s}^{-1}\right]$	Density, N_e $\left[\text{m}^{-3}\right]$
Indium Tin Oxide [7]	45	4×10^{26}
Antimony Tin Oxide [13]	9.7	1.26×10^{26}
Titanium Indium Oxide [14]	80	8×10^{26}
Gallium Zinc Oxide [15]	13	1×10^{26}

Table 3. Simulation and empirical results for the antenna radiation efficiency, e_r, with $\sigma = 2.6\times10^5$ S/m, $h = 2.3$ mm, and $W = 7.5$ mm.

Antenna Thickness, t	Empirical e_r	Simulation e_r
$t = 0.5$ μm	6.4%	10.0%
$t = 1.2$ μm	28.3%	25.8%
$t = 3.0$ μm	70.3%	53.2%

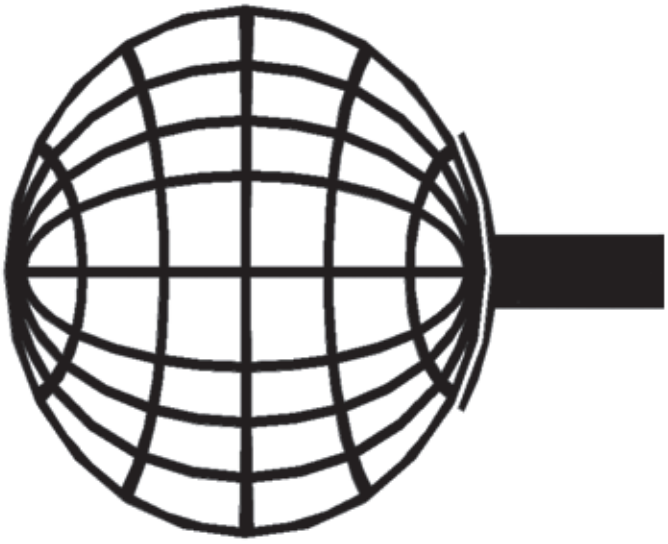

Figure 10. A circular see-through microstrip-patch antenna.

$R_a = 50\,\Omega$, by varying their width and length. The radiation efficiency in this case was calculated as $e_r = R_a/(R_a + R_s)$, and is shown in Figure 8 for an electron mobility of $\mu_e = 50\ \text{cm}^2\text{V}^{-1}\text{s}^{-1}$, and shown in Figure 9 for $\mu_e = 100\ \text{cm}^2\text{V}^{-1}\text{s}^{-1}$. The thickness, *t*, of the indium tin oxide deposition was 1.2 μm, in order to achieve transparencies of 50% to 68%, as seen in Figure 6, and transparencies of 70% to 80%, as seen in Figure 7.

These antennas had very poor radiation efficiencies at frequencies below 2 GHz. Efficiencies of more than 20% were achieved for frequencies above 5 GHz in the highest-mobility case in Figure 9. It is important to note that an electron mobility above $\mu_e = 100\ \text{cm}^2\text{V}^{-1}\text{s}^{-1}$ is very hard to achieve, and further materials development should be done to improve the electron mobility of transparent conducting oxides. The literature [7] has suggested that novel materials, such as titanium-doped indium oxide, could provide mobilities higher than $\mu_e = 50\ \text{cm}^2\text{V}^{-1}\text{s}^{-1}$. Table 2 gives a sample of different transparent-conducting-oxide materials and their respective μ_e and N_e values. If the ground plane is also transparent, the radiation efficiency, e_r, would substantially drop due to ground surface resistance, R_g, so mobility would become even more critical.

The results from Equation (14) were compared to full-wave numerical simulation results using CST *Microwave Studio*™. Good agreement was seen, as shown in Table 3.

One method of improving efficiency involves the placement of high-conductivity materials, such as copper, in areas of high current density [6]. This technique claims to improve transparent patch antenna efficiencies up to 30%, and could be used to improve transparent-conducting-oxide antenna efficiencies.

An alternative to transparent-conducting-oxide transparent antennas is meshed antennas [3], made from non-transparent conductors. These antennas are able to achieve effective transparencies by reducing the metallic area, while still retaining much of the electrical size and performance of a solid patch. These meshed patches have achieved transparencies of up to 80% while maintaining approximate radiation efficiencies of up to 60% [3]. It is also important to note that the ground and skin-depth effects are minimal for these antennas, due to copper's high free electron density ($N_e = 8.46\times10^{28}\ \text{m}^{-3}$) and electron mobility ($\mu_e = 44\times10\ \text{cm}^2\text{V}^{-1}\text{s}^{-1}$). Unlike antennas made out of transparent conducting oxides, see-through antennas do not require thin depositions, and can even be deposited inexpensively with metallic inkjet printing [16].

6. Conclusion

Transparent and conductive antennas are limited by intrinsic properties. Factors such as thin-film depositions smaller than 2μm create severe skin-effect losses that deeply influence antennas at microwave frequencies. When transparent-conducting-oxide materials are used for microstrip-patch design, the losses might increase by a factor of four, caused by a deformation of the current density around the patch and ground. Further studies may be required on the effects of transparent conducting oxides for different antennas such as wire antennas, slot antennas, and reflectarray applications. The feasibility of a high efficiency lies in the transparent conducting oxide's material properties, which seem to be restricted by the intrinsic limitations of transparent conducting oxides. However, if higher electron mobilities, μ_e ($>100\ \mathrm{cm^2V^{-1}s^{-1}}$), are achieved, then perhaps transparent antennas might turn into viable commercial products.

7. Acknowledgement

The authors would like to thank Dr. Michael Scarpulla, University of Utah, and Dr. Reyhan Baktur, Utah State University, for their helpful comments. This work was supported in part by grant 0801453 from the National Science Foundation.

8. References

1. R. Gordon, "Criteria for Choosing Transparent Conductors," *MRS Bulletin*, August 2000.

2. N. Guan, H. Furuya, D. Delaune, and K. Itao, "Antennas Made of Transparent Conductive Films," *PIERS Proceedings Online*, **4**, 1, 2008.

3. T. Turpin and R. Baktur, "Integrated Solar Meshed Patch Antennas," *IEEE Antennas and Wireless Propagation Letters*, **8**, 2009, pp. 693-696.

4. N. Outleb, J. Pinel, M. Drissi, and O. Bonnaud, "Microwave Planer Antenna with RF-Sputtered Indium Tin Oxide Films," *Microwave and Optical Technology Letters*, **24**, 1, 2000, pp. 3-7.

5. M. Bourry, M. Sarret, and M. Drissi, "Novel ITO Alloy for Microwave and Optical Applications," 48th Midwest Symposium on Circuits and Systems, **1**, August 2005, pp. 615-618.

6. H. J. Song, T. Y. Hsu, D. F. Sievenpiper, H. Hsu, J. Shaffner, and E. Yasan, "A Method for Improving the Efficiency of Transparent Film Antennas," *IEEE Antennas and Wireless Propagation Letters*, **7**, 2008, pp. 753-756.

7. A. Porch, D. V. Morgan, R. Perks, M. Jones, and P. P. Edwards, "Electromagnetic Absorption in Transparent Conducting Films," *Journal of Applied Physics*, **95**, 9, May 2004, pp. 4734-4737.

8. C. F. Bohren and D. R. Huffman, *Absorption and Scattering of Light by Small Particles*, New York, Wiley, 1883.

9. B. Streetman and S. Banerjee, *Solid State Electronic Devices, Sixth Edition*, Upper Saddle River, NJ, Pearson Prentice Hall, 2006.

10. C. Balanis, *Antenna Theory: Analysis and Design, Second Edition*, New York, 1996.

11. R. Faraji-Dana and Y. L. Chow, "The Current Distribution and AC Resistance of a Microstrip Structure," *IEEE Transactions on Microwave Theory and Techniques*, **38**, 9, September 1990, pp. 1268-1277.

12. A. Kerr, "Surface Impedance of Superconductors and Normal Conductors in EM simulators," NRAO Electronics Division, MMA Memo 245, January 1999.

13. X. Hao, J. Ma, D. Zhang, X. Xu, Y. Yang, H. Ma, and S. Ai, "Transparent Conducting Antimony-Doped indium Oxide Films Deposited on Flexible Substrates by RF Magnetron Sputtering," *Applied Physics A, Material Science and Processing*, **75**, 2002, pp. 397-399.

14. M. van Hest, M. Dabney, J. Perkins, and D. S. Ginley, "Titanium-Doped Indium Oxide: A High Mobility Transparent Conductor," *Applied Physics Letters*, **87**, 2005, pp. 32111-32500.

15. A. Tiburcio-Silver, A. Sanchez-Juarez, and A. Avila-Garcia, "Properties of Gallium-doped ZnO deposited onto Glass by Spray Pyrolysis," International Symposium on H-Fuel Cell Photovoltaic Systems, **55**, 1-2, 1998, pp. 3-10.

16. J. Saberin, C. Furse, T. Yasin, and R. Baktur, "Passive Feed Methods for Meshed Antennas," IEEE International Symposium on Antennas and Propagation, July 2010, Toronto, Canada.